A study of accuracy on numerical methods for nonuniform meshes

Anne M. Fernando*

Norfolk State University, Norfolk, Virginia, 23504

and

Fang Q. Hu[†]

Old Dominion University, Norfolk, Virginia, 23529

Abstract It is well-known that errors in modified wave number and modified temporal amplification factor, or modified frequency, lead to numerical dispersion and dissipation errors. In this paper, we try to answer the question, that given a numerical solution of the convective wave equation, how well can we recover the modified wave number and modified frequency of the spatial and temporal schemes? While a regular Fourier analysis in space or time assumes a uniform mesh, the computationally inferred modified wave number and modified frequency can be applied to nonuniform meshes. The essential formulas for finding computationally inferred modified wave number and frequency are given. Validation examples with known analytical results are presented and discussed. Applications to wave propagation on nonuniform meshes, where analytical expressions for modified wave number and modified frequency are difficult to find, are also presented. As computational meshes in practical applications become increasingly nonuniform and unstructured, and the numerical algorithms increasing adaptive, methods such as the one presented in this paper that can provide quantitative assessment of numerical dispersion and dissipation errors for these schemes are increasingly needed.

I. Introduction

Propagation of linear wave packets is governed by the dispersion relation supported by the underlying governing equations and boundary conditions. When the partial differential equations are discretized, due to discretization errors, the theoretical dispersion relation is inevitably modified, giving rise to numerical dispersion and dissipation errors are often analyzed through the concept of modified wave number of the spatial schemes and modified temporal amplification factor of the time integration schemes. 5,9,17,18,21 Such an analysis is useful because it shows the resolution of the numerical scheme which in turn helps the design of suitable computational meshes as well as the interpretation of the numerical results. Indeed, there are a considerable amount of literature on the study of modified wave numbers and modified temporal amplification factors for numerical schemes.

While it is possible in many instances to find the analytical expressions for the modified wave number or modified amplification factor, there are still other cases where these expressions are not so easily available or even well defined. On the other hand, the effects of modified wave number or amplification factor are manifested in the numerical solution and it whould be possible to extract these information by examining the numerical solution itself. The present paper is an attempt to computationally infer modified wave number and modified temporal amplification factor by carefully post-processing the numerical solution.

^{*}Associate Professor, Department of Mathematics

[†]Professor, Department of Mathematics and Statistics, AIAA Associate Fellow

The problem of detecting dispersion and dissipation errors directly from the numerical solution has been studied previously. In [12], an Approximate Dispersion Relation (ADR) was defined for nonlinear shock capturing schemes by computing a sinusoidal initial condition for one time step and analyzing the numerical solution for modified wave number. This method has been recently applied to many studies on nonlinear schemes.^{2,6,7,13,16} A similar approach was also proposed independently by the current authors in [3] for finding the modified wave number of a Discontinuous Galerkin Method based Finite Difference (DGM-FD) scheme for linear problems. This method was later extended to two dimensional schemes for the study of anisotropic errors in [4]. While the method given in [12] computes the modified wave number for one sinusoidal wave at a time, the formulations given in [3,4] used an initial condition that has a broad spectrum. As a result, modified wave number was recovered for the full range of the wave numbers in one computation.

In this paper, we first examine more closely the technique of finding computationally inferred modified wave number as was formulated in [3]. Then, a new and extended formulation for extracting the temporal amplification factor, or modified frequency, of time integration schemes will be given. Both of the formulations are validated with known results for finite difference schemes and the Runge-Kutta time integration schemes. Since extracting the computationally inferred modified wave number and frequency requires only the numerical solution at a fixed time, it can be an effective tool for analyzing quantitatively the dispersion and dissipation errors of numerical methods on nonuniform meshes. In particular, spectral properties of a nonuniform spatial scheme and a nonuniform time step Runge-Kutta method are computed as examples of the the techniques developed in this paper.

II. Modified Wave Number

Consider the convective wave equation in one dimension,

$$\frac{\partial u}{\partial t} + \frac{\partial u}{\partial x} = 0 \tag{1}$$

with initial condition

$$u(x,0) = u_0(x) \tag{2}$$

The exact solution for (1) is

$$u_{exact}(x,t) = u_0(x-t) \tag{3}$$

To facilitate the ensuing analysis, we express the exact solution in the Fourier space as

$$u_{exact}(x,t) = \frac{1}{2\pi} \int_{-\infty}^{\infty} \hat{u}_0(k)e^{ikx - i\omega(k)t}dk$$
 (4)

where

$$\omega(k) = k \tag{5}$$

is the dispersion relation for equation (1) and $\hat{u}_0(k)$ is the Fourier transform of the initial condition,

$$\hat{u}_0(k) = \int_{-\infty}^{\infty} u_0(x)e^{-ikx}dx \tag{6}$$

The Fourier transform of $u_{exact}(x,t)$ is

$$\hat{u}_{exact}(k,t) = \hat{u}_0(k)e^{-i\omega(k)t} \tag{7}$$

There is actually no dispersion present in the solution of (1). Equation (7) shows that at time t, the Fourier component for wave number k should be modified by a factor $e^{-i\omega(k)t}$, or the phase of which is altered by an amount of $-\omega(k)t$.

Now consider a numerical solution to (1), $u^h(x,t)$, and its spatial Fourier component, $\hat{u}^h(k,t)$. If h is a measure of the grid spacing, the range of wave number for the numerical solution $\hat{u}^h(k,t)$ will be limited to $|kh| \leq \pi$.

In many instances, it is possible to derive an equation for $\hat{u}^h(k,t)$ as a semi-discrete equation in the form of

$$\frac{d\hat{u}^h}{dt} + ik^h\hat{u} = 0\tag{8}$$

In such cases, $k^h = k^h(k)$ is the *modified wave number* for given k. The modified wave number for many of the spatial schemes by the finite difference and finite element methods are well-known.^{17,21} Finding and analyzing the modified wave number is an active area of research.

When the semi-discrete equation (8) is solved exactly, we have

$$\hat{u}^{h}(k,t) = \hat{u}_{0}^{h}(k)e^{-ik^{h}t} \tag{9}$$

where $\hat{u}_0^h(k)$ is the discrete Fourier transform of the initial condition.

Equation (9) shows that, the Fourier component for wave number k is a modification of that of the initial condition by a factor of e^{-ik^ht} . In this regard, errors in the modified wave number k^h will lead to inaccuracies in the phase, and hence numerical dispersion and dissipation (when k^h is complex) errors.

As mentioned earlier, in many instances, analytical expressions for k^h as it appears in (8) may be derived analytically. However, when k^h is not easily known or defined, it is the notion of this paper that the modified numerical wave number of a scheme can be inferred from the numerical results, as we will demonstrate next.

Comparing the Fourier space expression of the numerical and exact solutions, following [3], we form the following expression

$$\phi(k) = -\frac{\ln\left(\hat{u}^h(k,t)/\hat{u}_{exact}(k,t)\right)}{it} \tag{10}$$

Then, assuming $\hat{u}_0^h(k) = \hat{u}_0(k)$ for a known initial condition $u_0(x)$ and following (7) and (9), we can see that $\phi(k)$ is the difference between the modified and the actual wave numbers:

$$\phi(k) = k^h - k \tag{11}$$

It is a simple matter to extract the modified wave number k^h as

$$k^h = k + \phi(k) \tag{12}$$

where $\phi(k)$ is computed by (10), provided an appropriate branch of the ln function is taken. Since expression (10) can be evaluated directly from computational results, equations (12) gives the *computationally inferred* modified wave number (CIMWN).

In summary, the steps for extracting the computationally inferred modified wave number are as follows:

- Step 1: Starting with an initial condition $u_0(x)$, compute solution to (1) at a fixed time t $u^h(x,t)$
- Step 2: By Discrete Fourier Transform, compute $\hat{u}^h(k,t)$
- Step 3: By Discrete Fourier Transform, compute $\hat{u}_0^h(k)$ and then $\hat{u}_{exact}(k,t) = \hat{u}_0^h(k)e^{-ikt}$
- Step 4, Compute $\phi(k)$ by (10) and k^h by (12)

We will illustrate the calculations next.

II.A. Central finite difference schemes

Consider an approximation of spatial derivative by the finite difference scheme,

$$\left[\frac{\partial u}{\partial x}\right]_{j} = \frac{1}{\Delta x} \sum_{j=-M}^{N} a_{\ell} u_{j+\ell} \tag{13}$$

When the above formula is applied to (1), it is well known that the modified wave number is

$$k^{h} = -\frac{i}{\Delta x} \sum_{\ell=-M}^{N} a_{\ell} e^{i\ell k \Delta x}$$
(14)

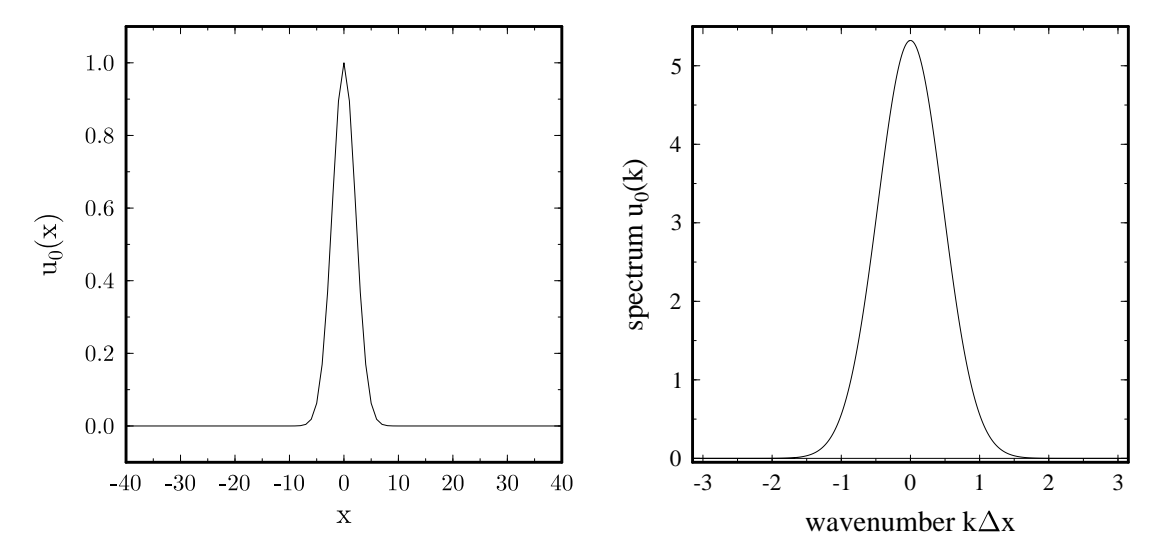


Figure 1. Initial condition $u_0(x)$ and its Fourier transform $\hat{u}(k)$.

For the examples in this section, we use an initial condition of the form

$$u_0(x) = e^{-x^2/b^2} (15)$$

Its Fourier transform is

$$\hat{u}_0(k) = \sqrt{\pi} b e^{-b^2 k^2 / 4} \tag{16}$$

For the case of $b = 3\Delta x$, $\Delta x = 1$, the graphs for $u_0(x)$ and $\hat{u}_0(k)$ are shown in Figure 1.

In Figure 2, the time evolution of the numerical solution is plotted, using the 6th-order central finite difference scheme as an example, namely, M=N=3 in (13). The computational domain extends from x = -500 to x = 500. The time integration scheme used is the low dissipation and low dispersion Runge-Kutta scheme LDDRK 56,⁵ with a very small time step, $\Delta t = 0.01$, such that no detectable errors are introduced in time integration. In this section, only the errors by the spatial discretization are studied. The errors by temporal schemes will be analyzed in the next section.

In Figure 2, a progressive view of the computational solution is shown. As the initial profile propagates to the right, due to inaccuracies in the modified wave number of the 6th-order central scheme, the dispersion errors are apparent. The particular initial condition has been chosen so that these errors are easily visible. In other words, since the initial condition entails a spatial spectrum that covers waves that are not well-resolved

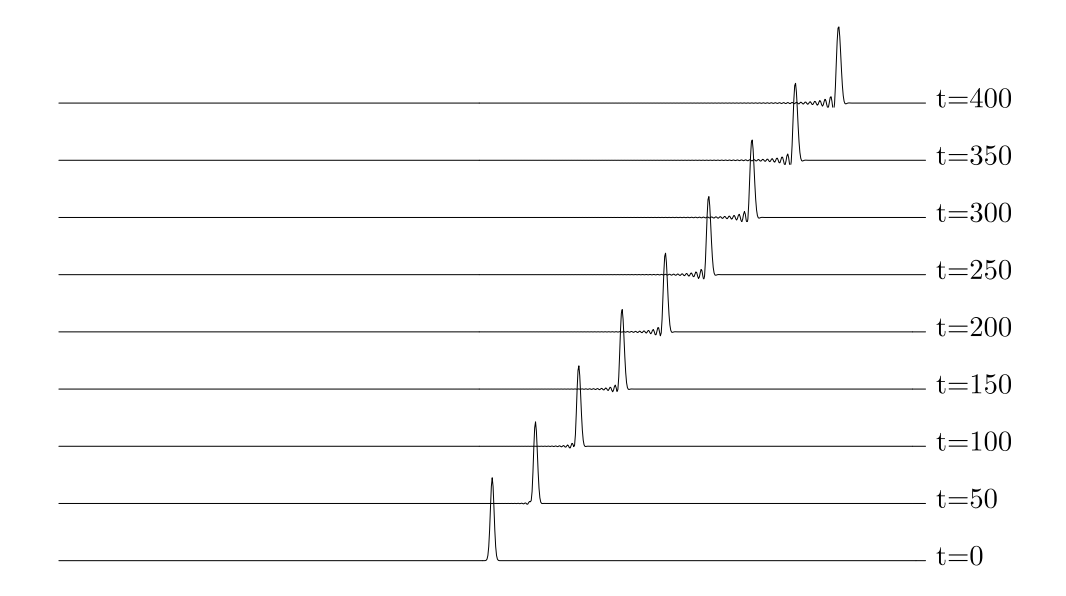


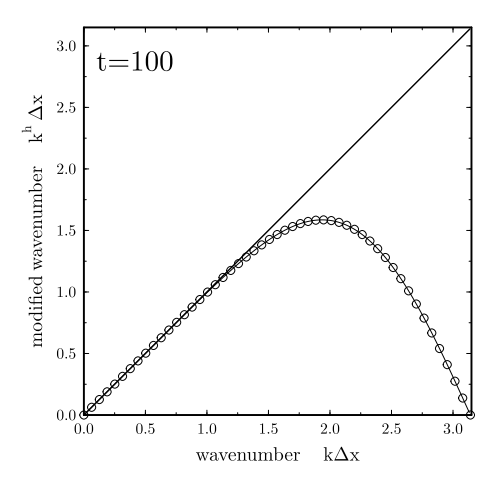
Figure 2. A progressive view of numerical solution at the time indicated.

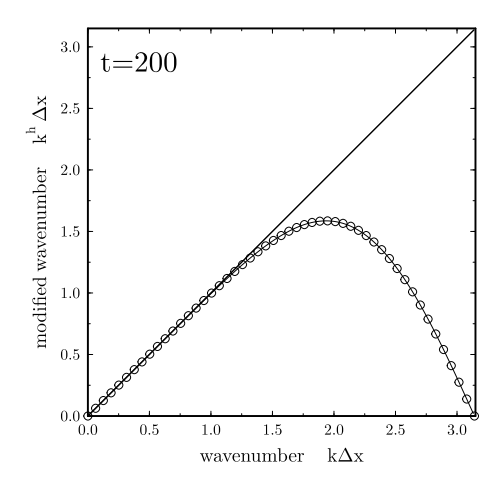
by the spatial discretization scheme used, these un-resolved waves propagate at the wrong speed as well as wrong direction. An analysis of the modified wave number can shed light on the dispersion errors found in the numerical solution and, in turn, provides guidance on the spatial resolution of the scheme. Such information makes knowing the modified wave number of a scheme critically important for wave propagation problems.

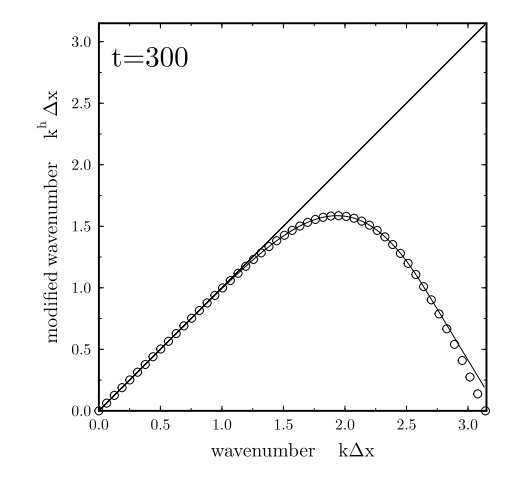
For central difference schemes, the modified wave number is well-known and given in (14). However, as we have discussed previously and will illustrate next, the modified wave number can also be recovered by post-processing the computational solution at a fixed time using the expressions developed in (10)-(12). In Figure 3, the modified wave number computed by formula (12) as well as that by the analytic expression (14) are plotted. Computational solutions at four different times, t = 100, 200, 300, 400, are used, giving four different cases in Figure 3. The computationally inferred modified wave number are shown in Figure 3 for all the four instances.

In the current example, as seen in Figure 3, when the numerical solutions at t=100 and 200 are used for computing and extracting the modified wave number of the scheme, excellent agreement with that given by the analytical formula (14) is observed for the entire wave number range of $|k\Delta x| \leq \pi$. We note that, in applying formula (10), appropriate branches of the log function should be taken so that $\phi(k)$ is continuous. On the other hand, when the solutions at t=300 or 400 are used, some deviations are seen in Figure 3 for wave numbers close to the $\pi/\Delta x$, i.e., the waves with a very short wavelength. The reason for this behavior can be understood as follows. As the plot of the modified wave number indicates, not only the short waves have highly inaccurate modified waves numbers, the short waves are also propagating in the negative direction, with a maximum negative slope of approximately -2.2. As a result, at time t=300 or 400, part of the short waves have left the computational domain, resulting in an impossibility of detecting their wave number. This situation is illustrated in Figure 4, which shows packets of short waves propagate in the negative direction. Figure 4 presents the same data as that in Figure 2, with the scales of the graphs being significantly zoomed in so that the very low amplitude short waves become visible.

This example shows that, to recover the modified wave number for the full range of the wave number, beware of the negatively propagating waves which may exit the computational domain sooner than the main wave







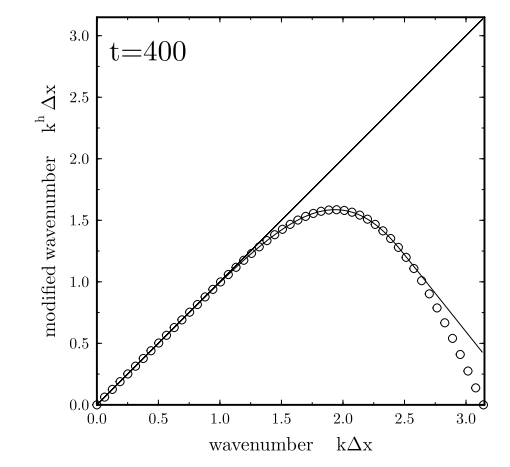


Figure 3. Computationally inferred modified wave number using the numerical solution at four different times as indicated.

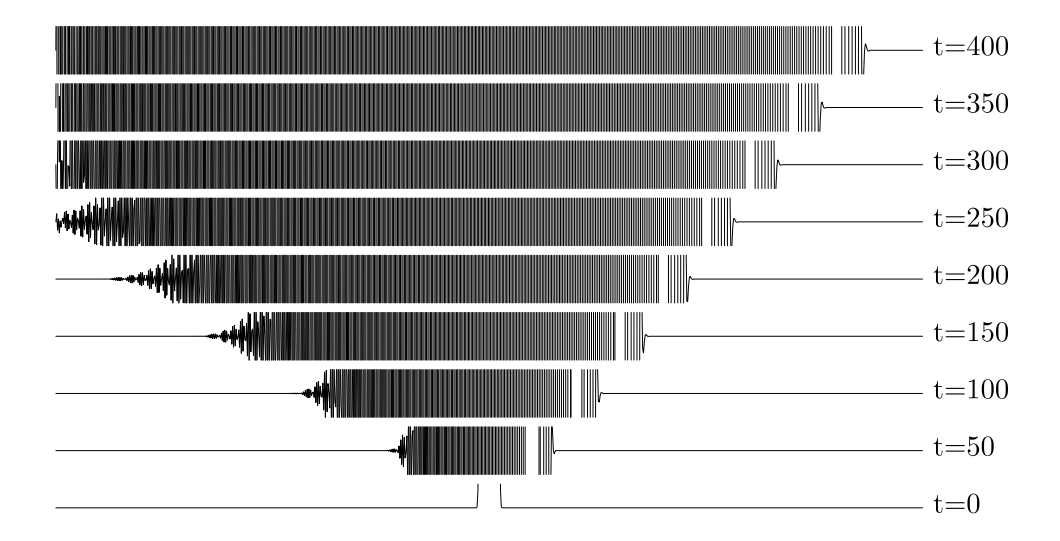


Figure 4. Numerical solution at indicated time, in magnified scale showing the negatively propagated waves.

signal. On the other hand, when waves of all wave numbers are present in the computational domain, the analytically predicted modified wave number does get accurately recovered, independent of the time when the solution is taken and the initial condition used.

In Figure 5, the computational inferred modified wave numbers for the 4th-, 6-th and 8-th central difference schemes are plotted with excellent matches with the analytical values in all the cases.

II.B. Upwind-biased finite difference schemes

In this section, we consider the modified wave number for non-central, upwind-biased, finite difference schemes. When $M \neq N$ in (13), the modified wave number will be complex, as a result, numerical dissipation is introduced in the non-central schemes. We will show again, by applying the formulas developed in (10)-(12), the modified wave number, both the real and imaginary parts, can be extracted and recovered.

In Figures 6 and 7, we show the computationally inferred modified wave number for two upwind-biased schemes, namely, M=3 and N=2, in circles, and M=3 and N=1, in squares. The real part of the modified wave number is shown in Figure 6 and the imaginary part is shown in Figure 7. Four cases of modified wave number extractions are considered, with the computational solution used being at t=5, 10, 20 and 50, respectively. For the results given by the solution at t=5, the modified wave number is recovered fully, for both the real and imaginary components. A close-up view is shown in Figure 8. Again, the analytic results for the modified wave number is plotted for comparison. However, the non-central scheme is dissipative, the larger the wave number the higher the dissipation rate. As the time for solution increases, the short waves are rapidly damped and becomes UN-detectable in the computational solution. For results using the solutions at t=10, 20, and 50, part of the short waves can not be recovered as shown in Figures 6 and 7.

III. Time integration errors and modified frequency

When the semi-discrete equation (8) in the Fourier space is solved numerically, instead of exactly, additional errors are introduced during the numerical time integration. We denote and rewrite the numerical solution

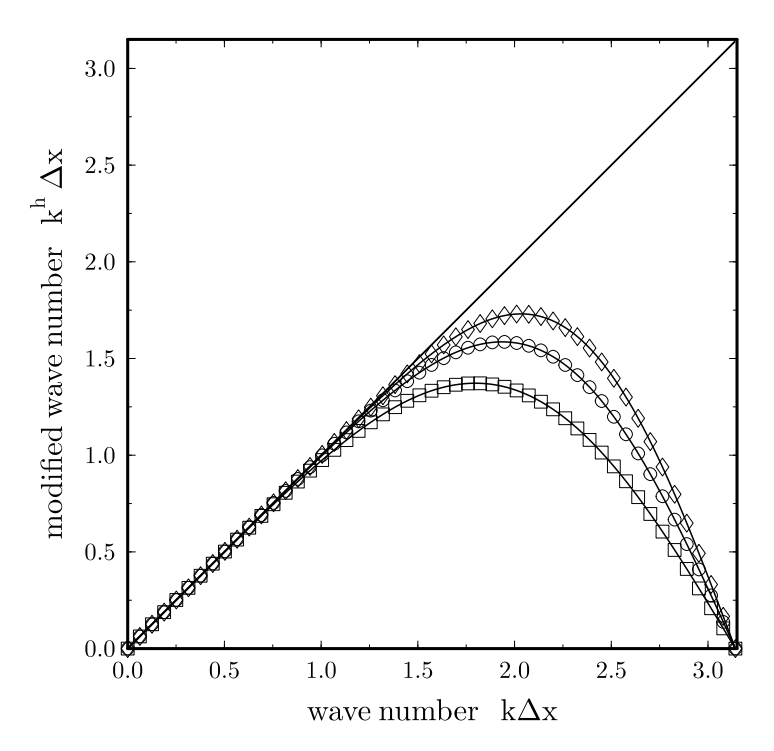


Figure 5. Computationally inferred modified wave number for central finite difference schemes of order 4 (square), 6 (circle) and 8 (diamond).

obtained by a time integration scheme of time step Δt as

$$\hat{u}^{h,\Delta t}(k,t) = \hat{u}_0(k)e^{-i\omega^h t} \tag{17}$$

Cast in the form shown above, ω^h will in general not be the same as k^h (Note the wave speed here is c=1). The difference of ω^h and k^h will depend on the accuracy of the time integration scheme and the time step Δt used. Often, the quantity

$$\lambda = e^{-i\omega^h \Delta t}$$

is called the amplification factor of the time integration scheme. Here, ω^h will be referred to as the modified frequency. In general, we have

$$\omega^h = \omega^h(k^h, \Delta t) \tag{18}$$

i.e., ω^h will be dependent on k^h and Δt , with the limiting case being $(\Delta t \to 0)$

$$\omega^h(k^h, 0) = k^h \tag{19}$$

We now form and analyze the expression $\theta(k, \Delta t)$ defined below:

$$\theta(k, \Delta t) = -\frac{\ln\left(\hat{u}^{h, \Delta t}(k, t)/\hat{u}_{exact}(k, t)\right)}{it}$$
(20)

Applying (17) and (7), we find that

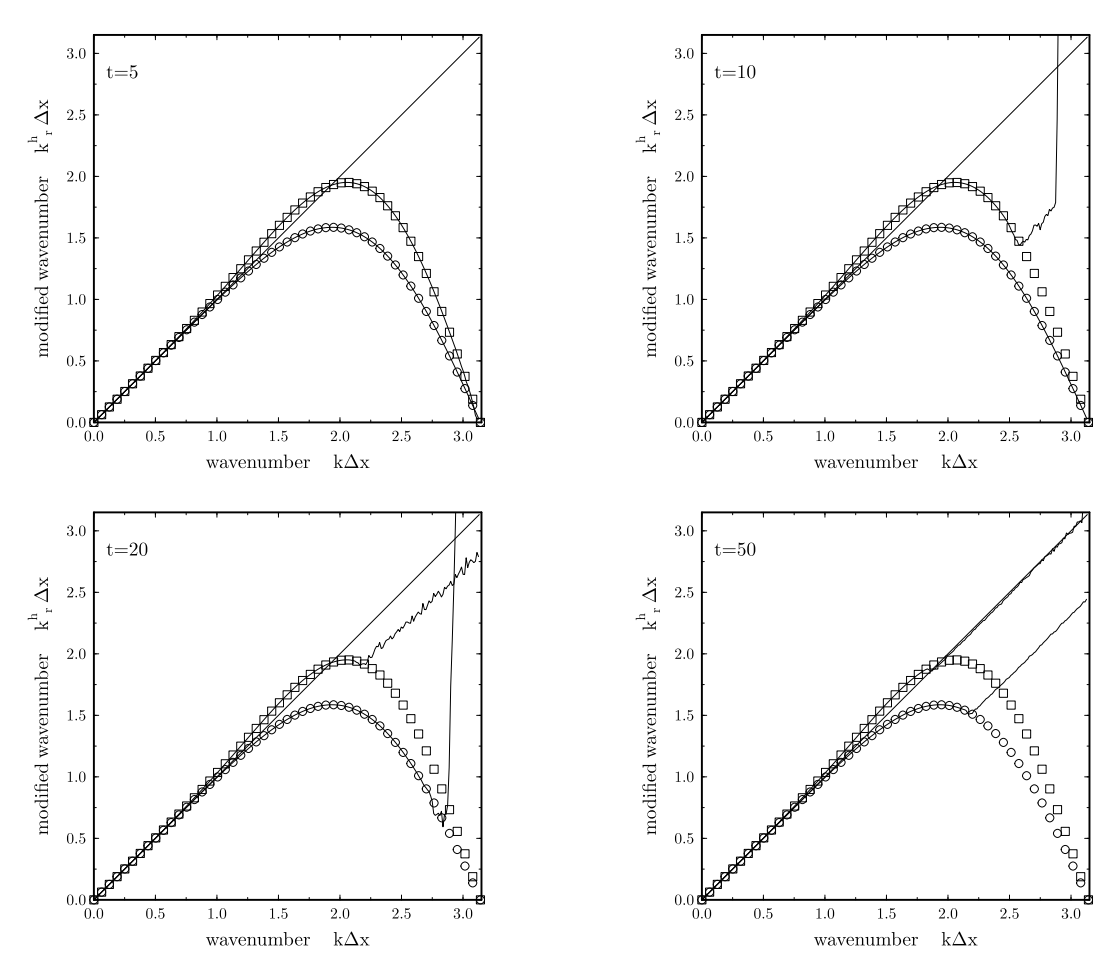


Figure 6. Computationally inferred modified wave number for upwind-biased schemes, for the real part. Circle: M=3, N=1; Square: M=3, N=2.

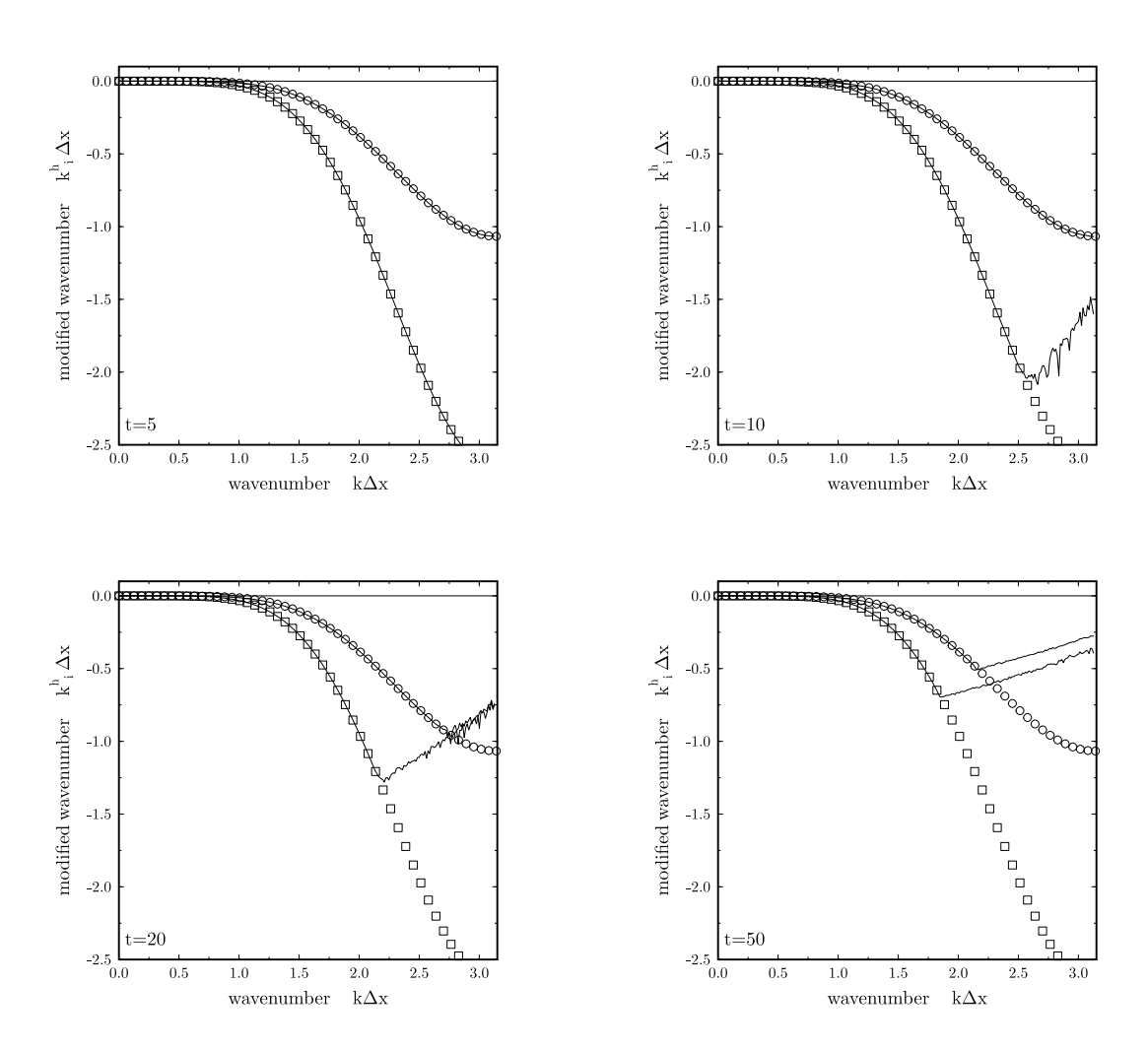
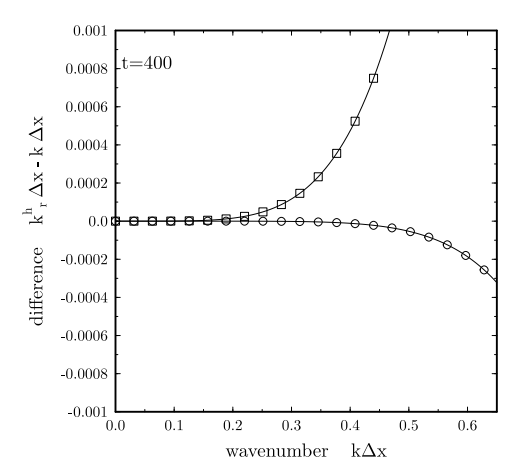


Figure 7. Computationally inferred modified wave number for upwind-biased schemes, for the imaginary part. Circle: $M=3,\ N=1;$ Square: $M=3,\ N=2.$



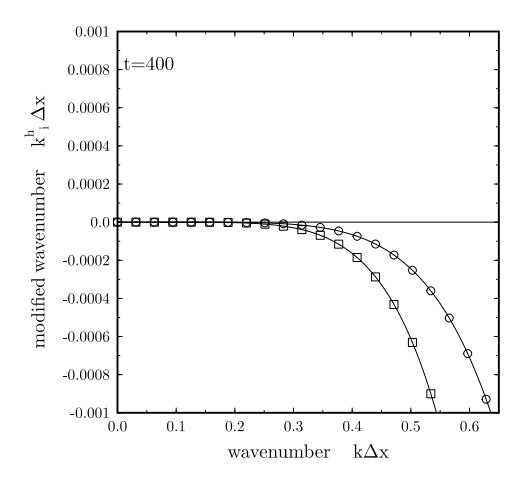


Figure 8. A close-up view of the computationally inferred modified wave number for upwind-biased schemes, for the real (left) and imaginary (right) parts. Circle: M = 3, N = 1; Square: M = 3, N = 2.

$$\theta(k, \Delta t) = \omega^h(k^h, \Delta t) - k \tag{21}$$

Equation (21) entails the accumulated error of both the spatial and temporal discretization schemes. The above can further be written as

$$\theta(k, \Delta t) = \omega^h(k^h, \Delta t) - k^h + k^h - k = \omega^h(k^h, \Delta t) - k^h + \phi(k)$$
(22)

where $\phi(k)$ is the error in modified wave number given in (10). As a result, the dispersion and dissipation errors due to the time integration scheme can be isolated and determined by the following expression:

$$\psi(k^h, \Delta t) = \omega^h(k^h, \Delta t) - k^h = \theta(k, \Delta t) - \phi(k)$$
(23)

The real and imaginary parts of $\psi(k^h, \Delta t)\Delta t$ represents the temporal dispersion and dissipation errors, respectively, per time step. Alternatively, $\psi(k^h, \Delta t)$ can also be computed as

$$\psi(k^h, \Delta t) = -\frac{\ln\left(\hat{u}^{h, \Delta t}(k, t)/\hat{u}^h(k, t)\right)}{it}$$
(24)

where $\hat{u}^h(k,t)$ is the Fourier transform of the nucrical solution $u^h(x,t)$ that was computed separately using a small Δt at which the temporal error is negligible.

In summary, the steps for extracting the temporal dissipation and dispersion errors and the modified frequency are as follows:

- Step 1: Compute the spatial modified wave number errors function $\phi(k)$ as described in the previous section;
- Step 2: Compute solution at time t using a fixed time step Δt and, by Discrete Fourier Transform, compute $\hat{u}^{h,\Delta t}(k,t)$
- Step 3: By Discrete Fourier Transform, compute $\hat{u}_0^h(k)$ and then $\hat{u}_{exact}(k,t) = \hat{u}_0^h(k)e^{-ikt}$
- Step 4, Compute $\theta(k, \Delta t)$ by (20) and $\psi(k^h, \Delta t)$ by (23)

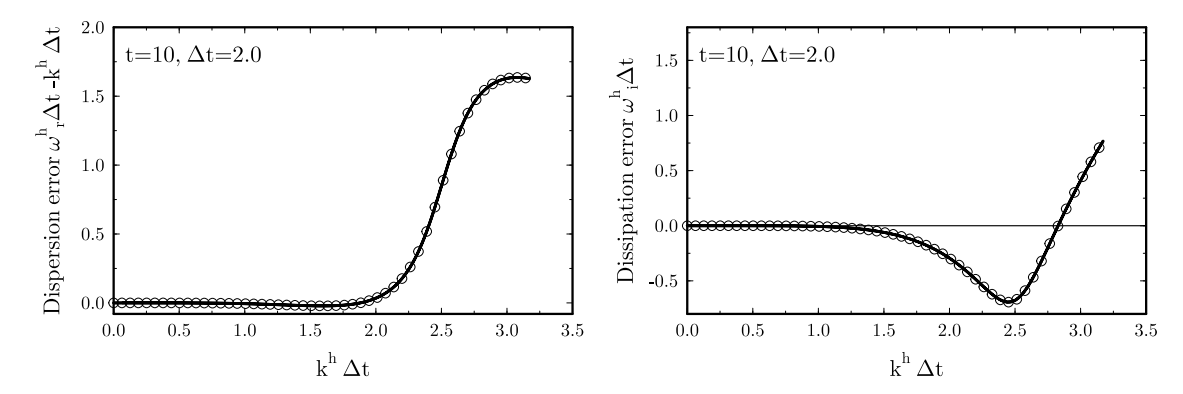


Figure 9. Computationally inferred modified frequency of the classical 4 stage 4th-order Runge-Kutta scheme.

We note that the fact that the expression given in (20) contains both the temporal and spatial dispersion errors has been well-known in the literature. Optimizations that are aimed to reduced the combined errors have been conducted in [1,14,15,20].

In Figure 9, we show the computationally inferred temporal dispersion and dissipation errors extracted from a solution at t=10 using the classical 4 stage 4th-order Runge-Kutta scheme with a time step $\Delta t=2.0$. The spatial discretization is that of the 4th-order central difference scheme. Since the temporal error has been separated from the spatial errors, the results for $\psi(k^h, \Delta t)$ is not dependent on the choice of the spatial discretization scheme used. The modified frequency for the classical Runge-Kutta schemes is well-known (Appendix). Compared to the theoretical predictions, the dispersion and dissipation errors are fully and accurately recovered by the procedures described in (20) and (23). We note that, the time step taken is actually beyond the stability limit of the 4th-order Runge-Kutta scheme. Interestingly, using the solution at t=10, the linear amplification factor of the time integration scheme is fully recovered, even for the amplified frequencies, i.e., those in Figure 9 that goes beyond the 4th-oder Runge-Kuta stability limit which is approximately at $k^h \Delta t = 2.83$.

The exponentially growing waves, as well as the exponentially damped waves, eventually will become either exceedingly large or undetectably small as the solution progresses. In Figure 10, the computationally inferred amplification factors obtained using the solutions at t=10 and t=200 are shown, where the time step, $\Delta t=1.5$, is within the stability limit. While the results provided by the solution at t=10 are valid for the full range of frequencies, those by the solution at t=200 lost validity for the high frequencies due to the high damping rate there. As a practical matter, however, information for modified frequencies that are within or close to the accuracy range is not subject to this loss because of the low damping rate of resolved waves.

We have also verified that the computationally inferred amplification factor is independent of the time step Δt used and the time when the computational solution is used. The choice of Δt affects only the range of the non-dimensional frequency which is limited to $k_{max}^h \Delta t$.

IV. Nonuniform spatial meshes

In the preceding sections, methods to extract directly from the numerical solutions the modified wave number and the modified frequency of the spatial and temporal discretization schemes have been formulated. The validity of the approach has been demonstrated by comparing the computationally inferred values with those of known analytical results. The utility of the proposed approaches lies in its application in schemes where analytical expressions for the modified wave number or modified frequency is difficult to derive, or even define. One such application is the analysis of numerical schemes for nonuniform meshes. While a regular Fourier analysis in space would assume a uniform mesh, or a pattern of mesh repeated periodically, the computationally inferred modified wave number or modified frequency can be more versatile and requires only a discrete Fourier transform of the numerical solution itself.

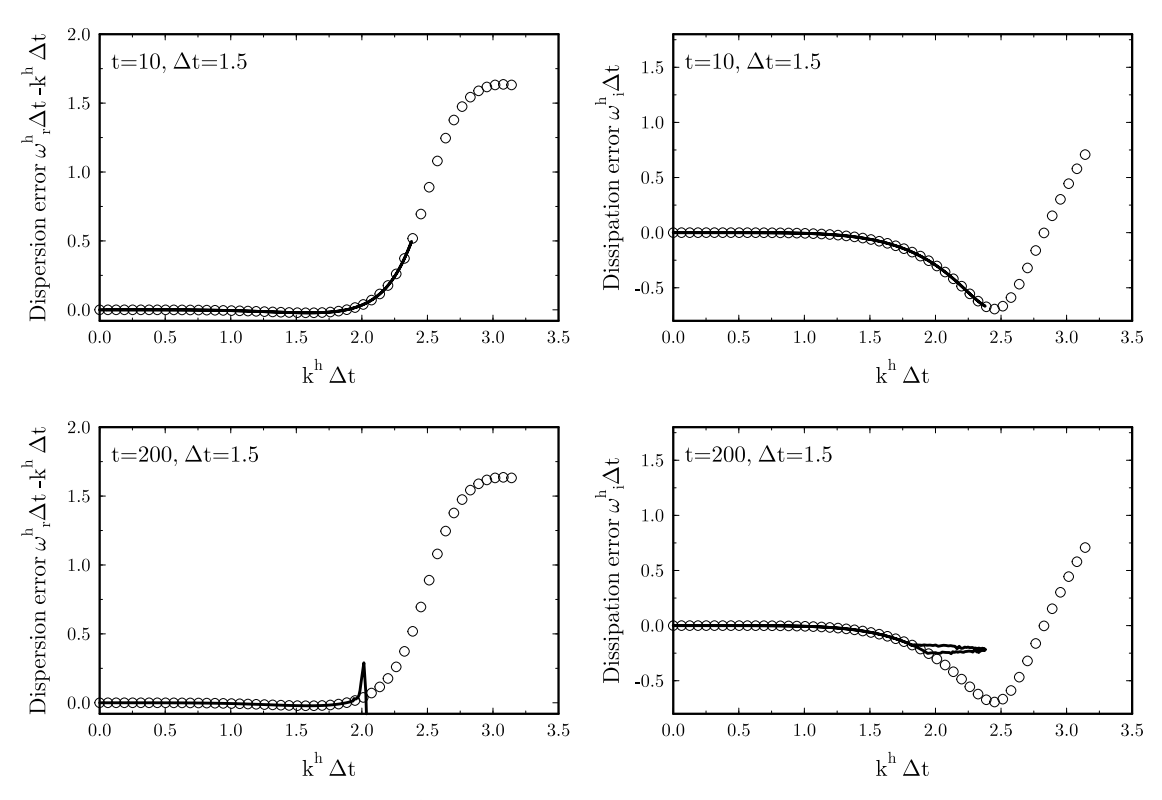


Figure 10. Computationally inferred modified frequency of the classical 4 stage 4th-order Runge-Kutta scheme using solutions at to different times.

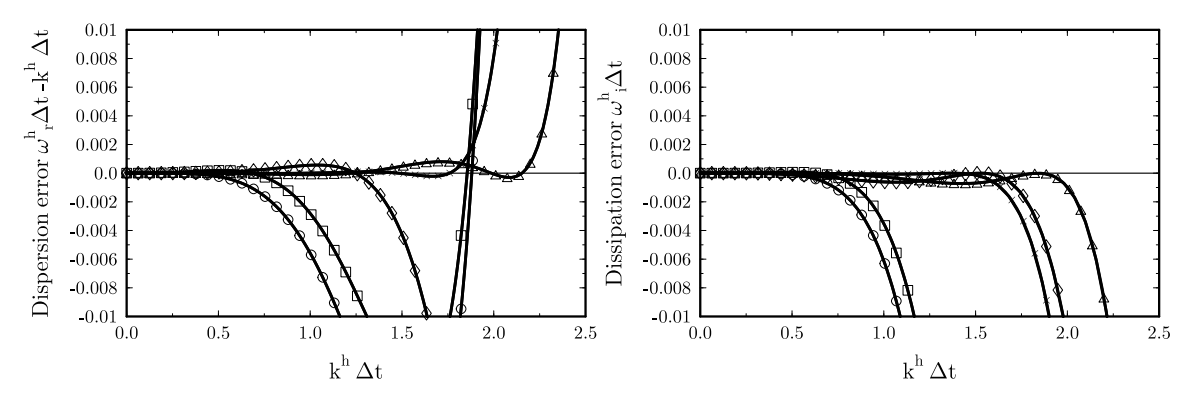


Figure 11. Computational inferred temporal dispersion and dissipation error for the classical 4th-order Runge-Kutta (\circ) , optimized LDDRK 4-stage (\Box) , 5-stage (\diamondsuit) , 4- and 6-stage alternating (\times) and 5- and 6-stage alternating (\triangle) schemes.

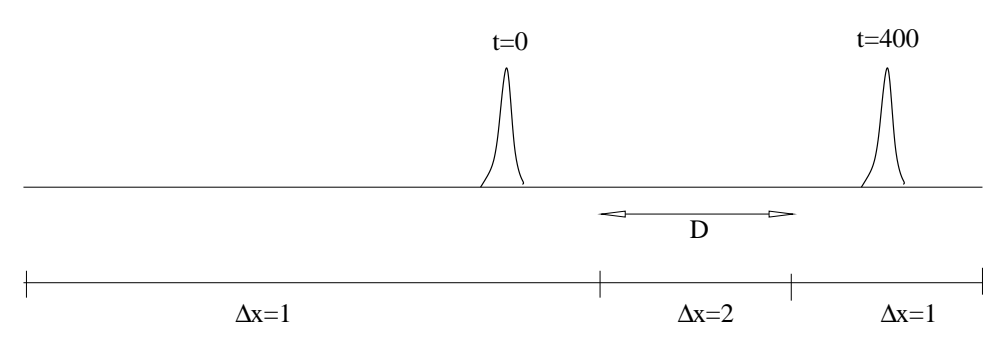


Figure 12. Schematic for a computation with nonuniform grid in one dimensional space.

In Figure 12, we show an example of computing the solution of (1) with a nonuniform grid. The spatial domain is [-500, 500] in which the grid spacing is $\Delta x = 1$ everywhere except in an interval denoted by D where the grid size is increased to $\Delta x = 2$. To study the effect of the grid coarsening on the modified wave number, the numerical solution st t = 400 is used to extract the modified wave number, after the pulse has propagated through the coarsened region.

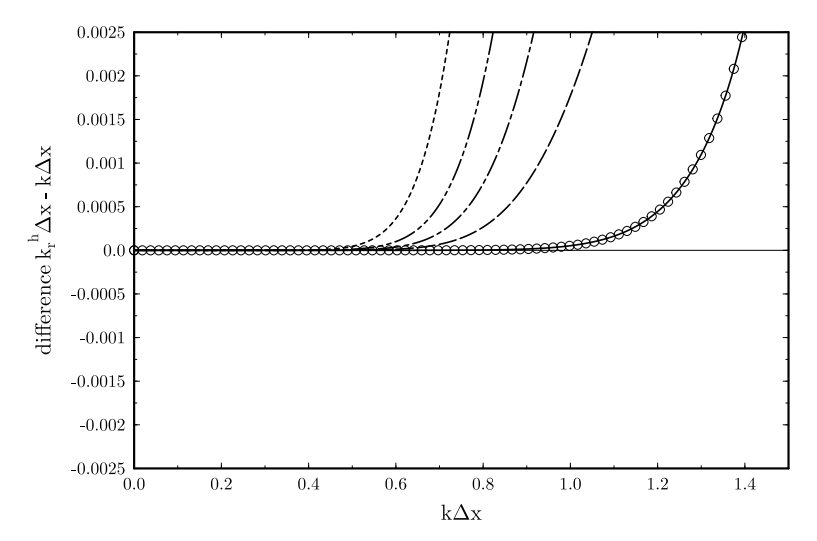


Figure 13. Effects on grid coarsening on the modified wave number. Grid size is doubled in interval D where D = [100, 300] (short dash), [100, 200] (dash-dot), [100, 150] (dash-dot) and [100, 120] (log dash). The results for a uniform grid without any coarsening are shown in the solid line.

The computationally inferred modified wave number is shown in Figure 13, using the solution at t = 400. In this example, the spatial discretization scheme is the Discontinuous Galerkin Method based Finite Difference (DGM-FD) scheme³ for its easy handling of variable grid spacings. The main purpose of the example is to show the ability of CIMWN in quantitatively assessing the effects of partial grid coarsening and mixed grid spacing on the resolution of the scheme. Figure 13 shows that while the error in modified wave number reduces as the region of coarsening narrows, from 200 grid points to 20 grid points, the reduction of the error is not linear. The effects on the overall resolution is still significant even if the grid coarsening is limited to 20 grid points.

V. Nonuniform time steps

In this section, we offer an example of the modified frequency for a Runge-Kutta scheme where the time step used is not uniform. It is well-known that, when a single time step is used uniformly, the allowable time step for the explicit Runge-Kutta scheme is restricted by the smallest mesh size in the entire computational domain. In situations where the mesh sizes are greatly uneven, this restriction on the explicit scheme can lead to a highly inefficient situation where a tiny time step is used even for regions where mesh size is larger. In such cases, using a single time step dictated by the smallest grid size in the whole domain leads to a significant slow-down in time marching.

In the part few years, a number of computational approaches have be proposed to reduce the impact of nonuniform spatial meshes on the time step. One such method is the implicit-explicit Runge-Kutta methods (IMEX RK).^{8,19} In this approach, an additive Runge-Kutta method is applied where the implicit scheme is applied on the fine meshes and explicit scheme is used on coarse meshes. Another approach is to use multiple time step sizes.¹⁷ In this section, a recently developed Non-Uniform Time Step Runge-Kutta (NUTS-RK) method is studied as an example.^{10,11} In this method, time step is not the same for all regions of the computational domain. A fine time step, Δt_f , is used in the zones where the grid spacing is small, and a coarse time step, Δt_c , is used in coarse zones, Figure 14.

For a system of differential equations expressed as

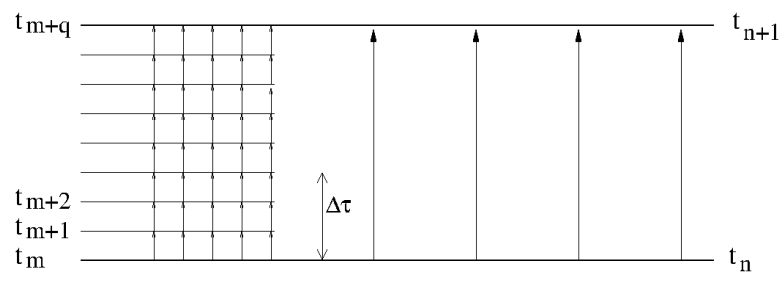


Figure 14. A schematic drawing illustrating the Non-Uniform Time Step Runge-Kutta scheme, for coupling between fine (left) and coarse (right) regions.

$$\frac{d\mathbf{U}}{dt} = \mathbf{F}(t, \mathbf{U}) \tag{25}$$

an s-stage explicit Runge-Kutta time integration system is expressed as

$$\boldsymbol{U}^{n+1} = \boldsymbol{U}^n + \sum_{i=1}^s b_i \boldsymbol{K}_i \tag{26}$$

where, for i = 1, 2, ..., s,

$$\boldsymbol{U}^{(i)} = \boldsymbol{U}^n + \Delta t \sum_{j=1}^{i-1} a_{ij} \boldsymbol{K}_j \text{ and } \boldsymbol{K}_i = \boldsymbol{F}(t + c_i \Delta t, \boldsymbol{U}^{(i)})$$
(27)

For the coupling of fine and coarse regions, the intermediate stage values needed for the fine region at any sub/inner fine time step $\Delta \tau$, Figure 14, can be computed from the values in the coarse region at t_n as

$$\begin{bmatrix} K_1^f \\ K_2^f \\ \vdots \\ K_s^f \end{bmatrix} = \boldsymbol{C} \boldsymbol{P}_{\Delta t_f} \boldsymbol{B}_{\Delta \tau} \boldsymbol{P}_{\Delta t_c}^{-1} \boldsymbol{C}^{-1} \begin{bmatrix} K_1^c \\ K_2^c \\ \vdots \\ K_s^c \end{bmatrix}$$
(28)

where super-scripts f and c denotes the values in the fine and coarse meshes respectively, and the matrices C, P and B can be precomputed and related to the coefficients of Runge-Kutta scheme used. ^{10,11} In particular, $P_{\Delta t_f}$ and $P_{\Delta t_c}$ are diagonal matrices and C is a lower triangular matrix related to the Runge-Kutta coefficients a_{ij} . Use of equation (28) avoids the need for temporal interpolation for the sub steps.

Similarly, the stage values needed for the coarse region from the fine region can be computed as

$$\begin{bmatrix} K_1^c \\ K_2^c \\ \vdots \\ K_s^c \end{bmatrix} = \mathbf{C} \mathbf{P}_{\Delta t_c} \mathbf{P}_{\Delta t_f}^{-1} \mathbf{C}^{-1} \begin{bmatrix} K_1^f \\ K_2^f \\ \vdots \\ K_s^f \end{bmatrix}$$

$$(29)$$

Further details are referred to [10,11].

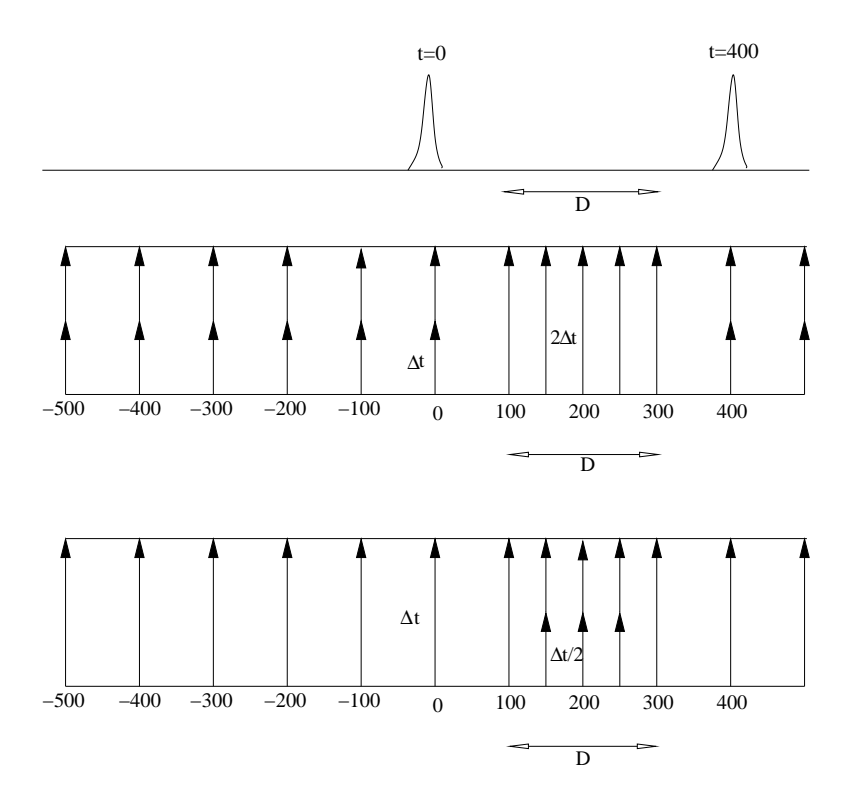


Figure 15. Schematic showing the nonuniform time steps in two cases considered.

Two cases of time integration with nonuniform time steps are considered in this example. In the first case, the time step is suddenly doubled in an interval D within in [100,300], Figure 15, and in the second case, the time step is reduced by a factor of 2 in interval D. In both cases, the coupling of the regions with different time steps is carried out by formulas given in (28) and (29). A pulse of (15) is initiated at time t=0. The numerical solution at t=400 is analyzed for modified frequency, after the pulse has propagated through the interval of nonuniform time steps. Hence, an analysis of the modified frequency at t=400 will show quantitatively the effects the NUTS-RK approach on the temporal dissipation and dispersion.

In Figure 16, temporal dissipation and dispersion errors extracted from the solution at t = 400 are plotted, for a series of the D intervals, D = [100, 300], D = [100, 200], D = [100, 150], and D = [100, 125]. Also plotted are the results when the time step is uniform without doubling of time steps taking place. Figure 16 shows that the dispersion and dissipation errors increase as the interval D widens, as expected. It is also seen that the coupling of the domains using (28) and (29) preserves the order of the temporal scheme.

In Figure 17, a reversed case is considered where the time step for interval D is reduced by half. Again, the coupling of coarse and fine regions is done through the NUTS-RK methods. The effects of the coupling on the modified dissipation and dispersion errors are quantified in Figure 17. Also as expected, the dispersion and dissipation errors are reduced when part of the domain uses a finer time step. The NUTS-RK coupling also preserves the order of the temporal scheme.

VI. Conclusions

Essential formulas for finding computationally inferred modified wave number of spatial discretization schemes and the modified frequency of time integration schemes are developed and discussed in this paper. Validation examples with known analytical results are presented. It is found that the modified wave number or frequency can be fully recovered as long as the wave components are present in the numerical solution used for extraction. The formulas for computationally inferred modified wave number and frequency become ineffective when the wave components have already been completely damped or propagated out of the computational domain.

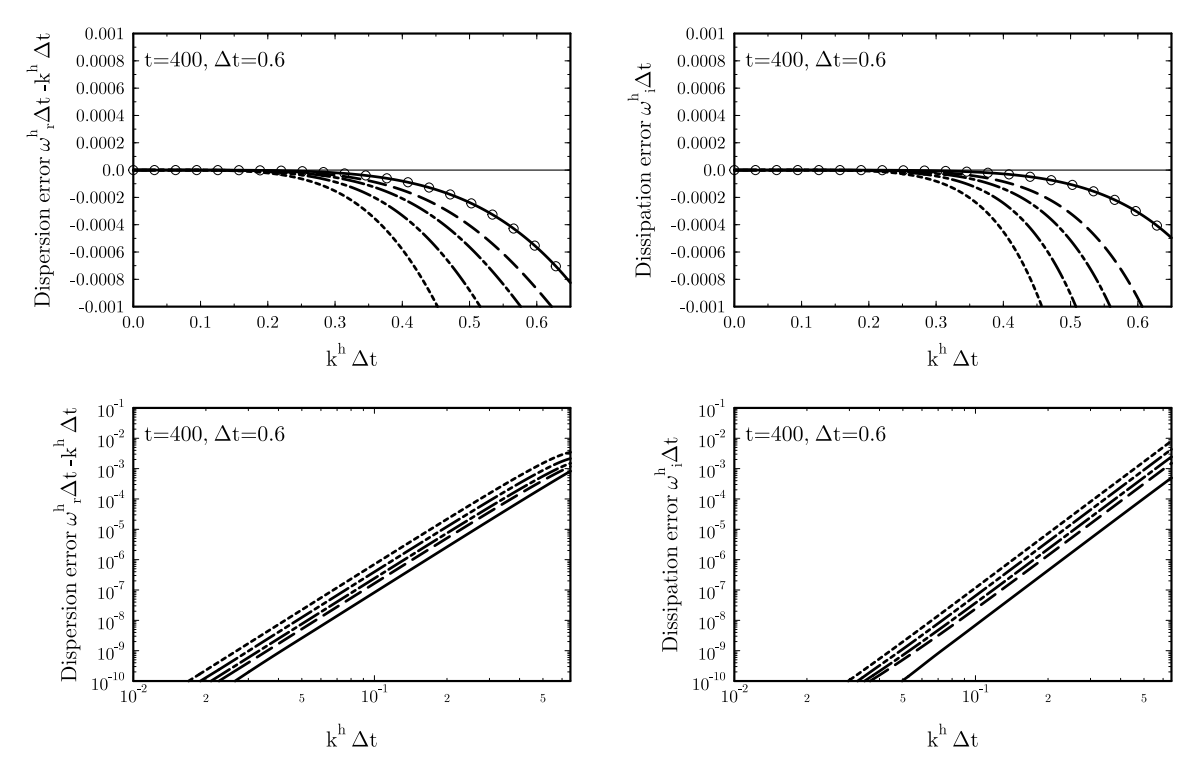


Figure 16. Computationally inferred temporal dispersion and dissipation errors. The time step is doubled in interval [100, 300] (short dash), [100, 200] (dash-dot-dot), [100, 150] (dash-dot) and [100, 125] (log dash). The symbol and solid lines are the analytical and numerical results of a uniform time step. Lower figures are the log-log plots, showing the preservation of the order.

It is emphasized that while a regular Fourier analysis in space would assume a uniform mesh, or a pattern of mesh repeated periodically, the computationally inferred modified wave number or modified frequency can be more versatile and requires only a discrete Fourier transform of the numerical solution itself. Applications to examples with nonuniform meshes show the capability of the presented formulas as a tool to study quantitatively the numerical dispersion and dissipation errors. As computational meshes in practical applications become increasingly nonuniform and unstructured, and the numerical algorithms increasing adaptive, methods such as the one presented in this paper that can provide quantitative assessment of numerical dispersion and dissipation errors for these schemes are increasingly needed.

ACKNOWLEDGMENT

This work is supported in part by NSF grant DMS-0810946.

Appendix

It is well-known that an s-stage Runge-Kutta scheme has an amplification factor that is a polynomial of the eigenvalue ω of the form

$$\lambda = 1 + c_1(-i\omega\Delta t) + c_2(-i\omega\Delta t)^2 + \dots + c_s(-i\omega\Delta t)^s$$

where $c_n = 1/n!$ for the classical schemes and ω is the actual frequency for the time integration. The analytical expression for the modified frequency is

$$\omega^{h} = \frac{i}{\Delta t} \ln \left[1 + c_1(-i\omega\Delta t) + c_2(-i\omega\Delta t)^2 + \dots + c_s(-i\omega\Delta t)^s \right]$$

The coefficients c_n may also be optimized to minimize $|\omega^h - \omega|$.

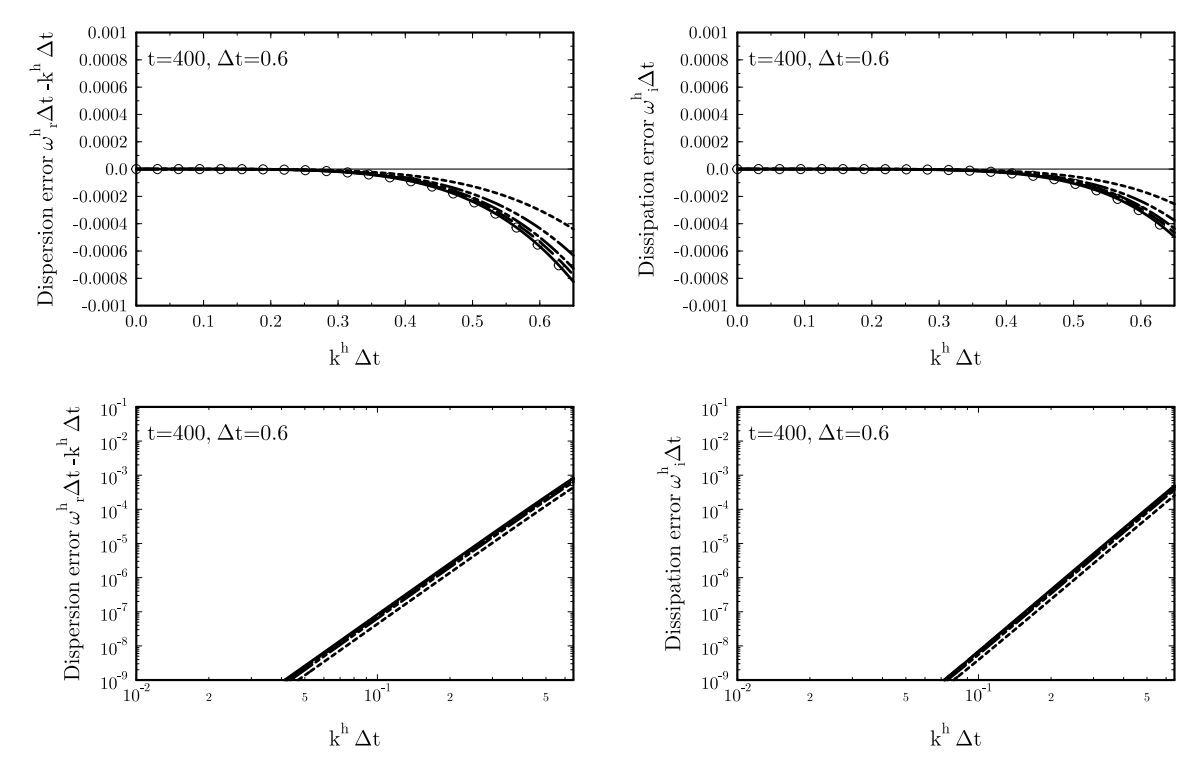


Figure 17. Computationally inferred temporal dispersion and dissipation errors. The time step is halved in interval [100, 300] (short dash), [100, 200] (dash-dot-dot), [100, 150] (dash-dot) and [100, 125] (log dash). The symbol and solid lines are the analytical and numerical results of a uniform time step. Lower figures are the log-log plots, showing the preservation of the order.

References

- ¹M. Bernardini and S. Pirozzoli, A general strategy for the optimization of Runge-Kutta schemes for wave propagation phenomena, Journal of Computational Physics, Vol. 228, 4182-4199, 2009.
- ²D. Fauconnier and E. Dick, On the spectral and conservation properties of nonlinear discretization operators, Journal of Computational Physics, Vol. 230, 4488-4518, 2011.
- ³A. M. Fernando and F. Q. Hu, DGM-FD: A finite difference scheme based on the discontinuous Galerkin method applied to wave propagation, Journal of Computational Physics, Vol. 230, 4871-4898, 2011.
- ⁴A. M. Fernando and F. Q. Hu, COMPUTATIONALLY-INFERRED NUMERICAL WAVE NUMBER FOR NON-UNIFORM GRIDS, The 21st International Congress on Sound and Vibration, July 13-17, 2014.
- ⁵F. Q. Hu, M. Y. Hussaini and J. Manthey, Low-dissipation and -dispersion Runge-Kutta schemes for computational acoustics. Journal of Computational Physics, Vol. 124, 177-191, 1996.
- 6 X.Y. Hu, N.A. Adams, Dispersion–dissipation condition for finite difference schemes, http://arvix.org/abs/1204.5088v1
- ⁷F. Jia, Z. Gao and W. S. Don, A spectral study on the dissipation and dispersion of the WENO schemes, Journal of Scientific Computing, Vol. 63, 49-77, 2015.
- ⁸A. Kanevsky, M. H. Carpenter, D. Gottlieb and J. S. Hesthaven, Application of implicit-explicit High-order Runge-Kutta methods to discontinuous Galerkin schemes, Journal of Computational Physics, Vol. 225, 1753–1781, 2007.
- ⁹S.K. Lele, Compact finite difference schemes with spectral-like resolution, J. Comput. Phys., Vol. 103, 16–42, 1992.
- ¹⁰L. Liu, X. D. Li and F. Q. Hu, Nonuniform time-step Runge-Kutta discontinuous Galerkin method for Computational Aeroacoustics, , Journal of Computational Physics, Vol. 229, 6874-6897, 2010.
- ¹¹L. Liu, X. D. Li and F. Q. Hu, Nonuniform-time-step explicit Runge-Kutta scheme for high-order finite difference method, Computers & Fluids, Vol 105,166-178, 2014
- ¹²S. Pirozzoli, On the spectral properties of shock-capturing schemes, Journal of Computational Physics, Vol. 219, 489-497, 2006.
- ¹³S. Pirozzoli, Performance analysis and optimization of finite-difference schemes for wave propagation problems, Journal of Computational Physics, Vol. 222, 809-831, 2007.
- ¹⁴M. K. Rajpoot, T. K. Sengupta and P. K. Dutt, Optimal time advancing dispersion relation preserving schemes, Journal of Computational Physics, Vol. 229, 3623-3651, 2010.
- ¹⁵J. Ramboer, T. Broechhaven, S. Smirnov and C. Lacor, Optimization of time integration schemes coupled to spatial discretization for use in CAA applications, Journal of Computational Physics, Vol. 213, 777-802, 2006.

- ¹⁶Z. Sun, L. Luo, Y. Ren and S. Zhang, A sixth order hybrid finite difference scheme based on the minimized dispersion and controllable dissipation technique, Journal of Computational Physics, Vol. 270, 238-254, 2014.
- 17 C. K. W. Tam, Computational Aeroacoustics, A Wave Number Approach, Cambridge University Press, 2012.
- ¹⁸C. K. W. Tam, J. C. Webb, Dispersion-relation-preserving finite difference schemes for computational acoustics, J. Comput. Phys., Vol. 107 262–281, 1993.
- ¹⁹Tanner B Nielsen, Mark H Carpenter, Travis C Fisher, Steven H Frankel, High-Order Implicit-Explicit Multi-Block Time-stepping Method for Hyperbolic PDEs, AIAA paper 2014-0770
- 20 T. Toulorge and W. Desmet, Optimal Runge-Kutta schemes for discontinuous Galerkin space discretization applied to wave propagation problems, Journal of Computational Physics, Vol. 231, 2067-2091, 2012.
- ²¹R. Vichnevetsky, J.B. Bowles, Fourier Analysis of Numerical Approximations of Hyperbolic Equations, SIAM, Philadelphia, 1982.